Diabatic states of a photoexcited retinal chromophore from *ab initio* many-body perturbation theory

Marcin S. Kaczmarski,* Yuchen Ma, and Michael Rohlfing
Department of Physics, University of Osnabrück, Barbarastrasse 7, 49076 Osnabrück, Germany
(Received 6 November 2009; revised manuscript received 1 March 2010; published 19 March 2010)

We investigate the diabatic electronic states of a photoexcited molecule within a diabatization method originally proposed by Baer [Chem. Phys. Lett. **35**, 112 (1975)]. A diabatization denotes a unitary transformation which allows for incorporating nonadiabatic effects into the quantum Hamiltonian, expressed in the adiabatic representation. A typical example is the treatment of avoided crossings in the potential-energy surface, for instance, in the case of the retinal chromophore. In this paper, we present analytical and numerical calculations for the diabatic states in the context of Green's-function-based *ab initio* many-body perturbation theory (density-functional theory plus GW method plus Bethe-Salpeter equation). We present the calculation of the adiabatic and diabatic lowest excited electronic states of the retinal chromophore molecule.

DOI: 10.1103/PhysRevB.81.115433 PACS number(s): 31.50.Gh, 71.15.−m, 82.20.Gk

I. INTRODUCTION

By separating the slow and fast degrees-of-freedom of the quantum Hamiltonian of nuclei and electrons, the Born-Oppenheimer approximation allows for a realistic description of many processes in condensed-matter systems. Within this approximation, one assumes that the nuclei move on a single potential-energy surface or, correspondingly, that the electrons adjust immediately to any change in the nuclear position. There are, however, situations in which this approximation may fail and nonadiabatic effects do play a role. Typical cases are given, for example, by chemical reactions caused by photoexcitation (such as photodissociation or photoisomerization). In this work, we investigate the photoisomerization process in the retinal chromophore in its protonated Schiff-base form.

The retinal chromophore is a light-absorbing polyene molecule in the rhodopsin protein. In the animal eye, visible light absorbed by the 11-*cis* form of the retinal chromophore causes its isomerization to the all-*trans* form, thus initiating an ultrafast chemical reaction which effectively converts the photon to an electrical signal activating the process of vision.[1] Another interesting case, which we consider in this paper, is the photoisomerization of retinal from *trans* to 13-*cis* in the bacterium *Halobacterium halobium*. Under anaerobic conditions, this bacterium produces bacteriorhodopsin—a protein which converts absorbed photon energy into an electrochemical gradient. This gradient pumps protons unidirectionally across the membrane in which the protein is located, thus forming a driving force for the synthesis of adenosine triphosphate (ATP).[2] The light-sensitive structure in bacteriorhodopsin is given by a retinal chromophore which is linked by a protonated Schiff base to the Lys-216-amino group of the protein. Upon absorption of a single photon, the all-*trans* form isomerizes to the 13-*cis* form. Figure 1 shows the chemical structure of the all-*trans* isomer of the protonated Schiff-base retinal (PSBR). For simplicity (and for facilitating the calculations to be discussed in this paper), we replace the chemical link to the protein by a saturating methyl group (right-hand side of Fig. 1).

Retinal is an aromatic system, with its double bonds forming large orbitals extending over the whole molecule. From these orbitals, electrons can be easily excited by light of the visible range of 400–800 nm wavelength. After this photoexcitation, the molecule can isomerize by rotating around one of the double bonds. Figure 1 illustrates one of these possibilities, i.e., a rotation around the bond between atoms 13 and 14, turning the all-*trans* form into the 13-*cis* isomer as it occurs in bacteriorhodopsin.

The photoisomerization of PSBR is often discussed within two competing models, as displayed in Fig. 2. This figure denotes schematically the ground state S_0 and the first two excited electronic singlet states S_1 and S_2 as a function of the twisting angle. The all-*trans* form (13-*cis* form) refers to a twist angle of 0° (180°). The *two-state* model would predict that a photoexcited electron causes a very fast torsional motion toward the minimum (at about 90°) of the S_1 excited-state potential-energy surface (PES) since the Franck-Condon region in this PES would be repulsive around 0°. This would lead directly to very fast movement into the active region (at about 90°), which should be accomplished within about 100–200 fs. From this configuration, the ground state S_0 (corresponding either to all-*trans* or 13-*cis*) would be reached within another ~500 fs, continuing the torsional motion through the avoided-crossing point between the PES of S_0 and S_1. The *three-state* model, on the other hand, assumes that the torsional movement along the reaction coordinate accesses a shallow well in the flat Franck-Condon region on the PES of S_1. This well would arise from the avoided crossing between the S_1 state and another excited

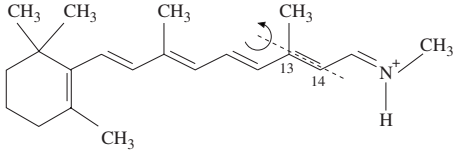

FIG. 1. Chemical structure of the all-*trans* isomer of the protonated Schiff-base retinal chromophore. The dashed line denotes the twist axis considered in this paper (referring to the isomerization between the all-*trans* and 13-*cis* configuration).

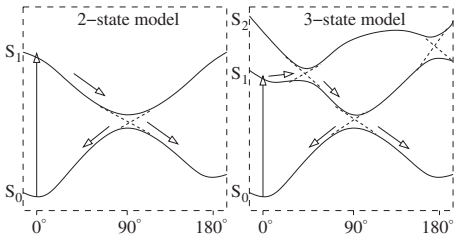

FIG. 2. Two commonly discussed models of the isomerization reaction path from all-*trans* at 0° to 13-*cis* at 180° of PSBR in bacteriorhodopsin.

state (S_2). As the result of this tumbling state, the reactive, steep region (between about 45° and 90°) would be reached later in time, and the twisted conformation at the second avoided-crossing point (at about 90°) would be reached in about 500 fs, i.e., significantly slower than in the two-state model. Both models have been supported both by theoretical and by experimental studies (see Ref. 3, and references therein for details). However, recent experimental data[4] seem to favor the three-state model, with a quantum yield for the photoisomerization reaction of about 0.64.[5]

In the Born-Oppenheimer approximation and the adiabatic representation, two or more adjacent PES may exhibit so-called *avoided crossings*, as indicated by the solid lines in Fig. 2. An avoided crossing would inhibit any electronic transitions between the two PESs as the reaction coordinate varies. Such inhibition is often not realistic and constitutes a significant failure of the Born-Oppenheimer approximation. A straightforward way to overcome such problems is to describe the so-called *nonadiabatic effects* (i.e., effects beyond Born-Oppenheimer) directly in the traditional adiabatic representation. This requires to evaluate two quantities, i.e., (i) the global PESs of the adiabatic states and (ii) the nonadiabatic coupling terms (NACTs) between them. The latter result from the action of the nuclear kinetic-energy operator on the electronic wave function. In practice, this implies that in the adiabatic representation, the quantum-dynamical calculation of the nonadiabatic process is pursued by substituting the molecular Hamiltonian into the Schrödinger equation. In here, a set of coupled differential equations must be integrated in time, including the calculation of the NACTs as the investigated reaction proceeds. Since the NACTs are formally given by the matrix elements of the nuclear derivative operator between electronic states, the calculation of them is a very demanding task.

In this work, we employ an alternative approach, i.e., the change in representation by an appropriate unitary transformation applied to the electronic and nuclear eigenstates. In this new *diabatic* representation, the derivative couplings between electronic states are rigorously removed or at least reduced to a minimum.[6] The electronic Hamiltonian matrix becomes nondiagonal, and the diagonal elements of it constitute *new* PESs which may now cross each other. Such diabatic PESs are illustrated in Fig. 2 as dashed curves. Diabatization has been applied traditionally in the context of quantum chemistry calculations, such as, e.g., the configuration-interaction (CI) method.[7] Diabatization is, however, not a unique method. Owing to the computational cost of quantum-chemical many-particle methods such as CI, several approximative methods have been suggested, leading to a *quasidiabatic* representation. These usually avoid the computation of the derivative couplings between states. Some of these approximations rely on the diagonalization of a so-called property matrix.[8] Others analyze the coefficients of the CI states and check for so-called dominant configurations in them, which should not change significantly as the reaction coordinate varies.[9]

The big advantage of working in the diabatic representation is given by a significant reduction in computational cost as compared to the adiabatic representation. In the adiabatic representation, the electronic wave functions depend on nuclear coordinates and therefore, one has to solve a set of coupled equations for the molecular wave function and calculate the first- and the second-order derivative of the electronic wave function with respect to all nuclear coordinates. In our approach, on the other hand, first we calculate only the first-order derivative along the reaction coordinate of interest and second we do it typically only for a few states of interest. Without this, staying at the BO approximation, one decouples nuclei and electronic degrees of freedom and the result is that the motion of the nuclei evolve separately in each electronic state without being affected by each other. This means that any kind of photoisomerisation and also quite a big number of photodissociation processes cannot be simply described.

In the present work, we propose a physics-motivated method to obtain the diabatic electronic states. Here we use many-body perturbation theory within the DFT-GW-Bethe-Salpeter equation (BSE) scheme to get an accurate description of the excited electronic states. We then apply a universal diabatization method proposed by Baer,[10,11] which we find most suitable in our approach. In particular, this method does not depend on any other additional assumptions.

The paper is organized as follows. In Sec. II, we briefly describe the diabatization scheme and its embedding in the GW-BSE method. In Sec. III, we investigate the photoisomerisation reaction of PSBR by discussing both adiabatic and diabatic electronic states of the molecule, taking into account the first two singlet excited states. Our findings are summarized in Sec. IV.

II. METHODOLOGY

In this section, we discuss all the indispensable theoretical components of the theory and provide the realization of Baer's diabatization scheme within the GW-BSE method.

A. General theory on the adiabatic representation and the diabatization scheme

Within the adiabatic representation, we write the molecular Hamiltonian of the system (consisting of nuclei and electrons) as the usual sum of the nuclear kinetic-energy operator T and the electronic Hamiltonian H_e. Consequently, from solving the electronic eigenvalue problem at fixed nuclei positions R, we obtain the adiabatic electronic eigenstates $\Psi_n(r,R)$ and eigenvalues ϵ_n. The molecular wave function ϕ

is constructed as an expansion in the complete orthonormal basis of electronic states Ψ_n,

$$\phi(r,R) = \sum_n \chi_n(R)\Psi_n(r,R), \tag{1}$$

where χ denotes the nuclear wave function. Substituting ϕ into the molecular eigenvalue problem, one arrives at the following familiar equation, expressed in the adiabatic representation and using a matrix form,

$$(\mathbf{T}+\mathbf{V})\mathbf{X}(R) = E\mathbf{X}(R). \tag{2}$$

Here, $\mathbf{V}$ denotes the diagonal matrix of the electronic adiabatic PESs and $\mathbf{X}$ is the vector of the nuclear wave functions. $\mathbf{T}$ is the matrix of the nuclear kinetic-energy operator in the electronic basis set, given more precisely as

$$\mathbf{T}_{mn}(R) = T(R)\,\delta_{mn} + \Gamma_{mn}(R). \tag{3}$$

The Γ_{mn} coefficients are the NACTs that arise from the action of the T operator on the Ψ_n states and contain the following derivative couplings between electronic states:

$$\tau^{(1)}_{mn} = \left\langle \Psi_m \middle| \frac{\partial}{\partial R} \Psi_n \right\rangle,$$

$$\tau^{(2)}_{mn} = \left\langle \Psi_m \middle| \frac{\partial^2}{\partial R^2} \Psi_n \right\rangle. \tag{4}$$

In the adiabatic approximation the off-diagonal elements of Γ are neglected, which corresponds to assuming that the nuclear kinetic energy is much smaller than that of the electrons. If one further assumes that also the diagonal components of Γ depend only weakly on the nuclear coordinates, one would neglect Γ completely and thus arrive at the common Born-Oppenheimer approximation.

Baer showed[10] that upon a suitable unitary transformation of the basis, Eq. (2) may be transformed into the diabatic representation. In this representation, the Γ_{mn} vanish and the matrix $\mathbf{T}$ of Eq. (3) becomes diagonal whereas the matrix $\mathbf{V}$ now acquires off-diagonal elements. This transformation is described by a matrix $\mathbf{A}$ which results from solving the differential equation,

$$\nabla\mathbf{A} + \tau\mathbf{A} = 0. \tag{5}$$

In here, the τ matrix of derivative couplings consists of the elements of $\tau^{(1)}$ of Eq. (4); τ is found to be anti-Hermitian.

Considering n electronic states, the diabatization can be performed, in practice, by utilizing the fact that $\mathbf{A}$ should be an orthogonal matrix. Therefore, it may be simply considered as a product of n-dimensional rotational sub matrices $\mathbf{Q}$,

$$\mathbf{A}(\theta_1,\theta_2,\ldots) = \prod_{i<j}^{n} \mathbf{Q}^{(ij)}(\theta_{ij}). \tag{6}$$

The n parameters θ_{ij} are the so-called *nonadiabatic mixing angles*. Equation (6) leads to a system of coupled differential equations of the same form as Eq. (5) for all n nonadiabatic mixing angles θ. Once all the mixing angles θ have been found, the following transformation gives the diabatic representation of the electronic Hamiltonian matrix:

$$W = \mathbf{A}^{\dagger}\mathbf{V}\mathbf{A}. \tag{7}$$

In here, the $\mathbf{V}$ matrix denotes the diagonal matrix of the adiabatic electronic states.

B. Analytical embedding in the DFT-GW-BSE scheme

In this section, we discuss how to calculate the excited electronic states in the adiabatic picture and how to evaluate the derivative couplings that are required to define the diabatization formulas. The excited state is taken as one electron-hole pair, which is generated when the system absorbs a photon. Since the molecule has a closed-shell (i.e., spin-singlet) electronic ground state, only singlet-to-singlet excitations are of relevance for light absorption. The electron-hole pair states and their excitation energies Ω_n result from the poles of the interacting two-particle Green's function, which we evaluate by means of the so-called GW-BSE method.[12] A practical scheme of solving for the poles is given by a diagrammatic expansion of the electron-hole propagator G_2 in terms of the scattering (or electron-hole interaction) kernel K. This approach, which is known as the BSE (Ref. 13) for G_2, may be briefly written in frequency space as

$$G_2(\omega) = G_2^{(0)}(\omega) + G_2^{(0)}(\omega)K(\omega)G_2(\omega), \tag{8}$$

with $G_2^{(0)}$ being the propagator of an electron and a hole as independent particles (given by a the product of two single-particle propagators, G_1, for the electron and the hole alone). In lowest order, the scattering kernel K consists of two terms, i.e., a bare-Coulomb-interaction exchange terms and a screened-Coulomb-interaction direct term. We evaluate the latter in the ring-diagram approximation for the polarization propagator [random-phase approximation (RPA)]. This evaluation of K was found useful first by Sham and Rice[14] and later by Strinati.[15]

Before evaluating Eq. (8), we have to solve the equation of motion for the one-particle propagator G_1, using Hedin's GW approximation[16] to the self-energy, i.e., $\Sigma = iGW$. Here W is the screened-Coulomb interaction, which we again evaluate at the RPA level. The eigenstates and eigenvalues thus obtained have the interpretation of the Landau quasiparticle states (describing both electron and hole states of the molecule). In practice, we deal with Σ as a perturbative correction to the single-particle states obtained from a preceding density-functional theory (DFT) calculation.[17]

For G_2, we mostly consider the case of forward propagation in time when calculating the particle-hole propagator within RPA. In practice, this means that the excited states Ψ_n can only be obtained by *creation* of an particle-hole pair, neglecting the possibility of destroying the pair. This restriction is known as the Tamm-Dancoff approximation (TDA) to the RPA states (see the discussion in Ref. 18). The excited states can thus be expressed as linear combinations of the particle-hole states,

$$|\Psi_n\rangle = \sum_v \sum_c A^n_{vc} a^{\dagger}_v b^{\dagger}_c |0\rangle, \tag{9}$$

where the first sum runs over all occupied single-particle states (i.e., holes) while the second sum runs over the empty

states (i.e., electrons). The $a_v^\dagger$ and $b_c^\dagger$ operators create the particle-hole pair; the $|0\rangle$ state denotes a single Slater determinant of the occupied valence states. Expressing the electron-hole amplitudes of G_2 according to Eq. (9) and inserting this into the BSE [Eq. (8)] results in the following eigenvalue problem:

$$(\epsilon_c - \epsilon_v)A_{vc}^n + \sum_{v'c'} K_{vc,v'c'}(\Omega_n)A_{v'c'}^n = \Omega_n A_{vc}^n. \quad (10)$$

In here, ϵ_c and ϵ_v are the quasiparticle energies of the occupied (hole) and unoccupied (electron) single-particle states, as obtained from the GW calculation. Solving the BSE yields the expansion coefficients A_{vc}^n and excitation energy Ω_n of each coupled electron-hole pair state n ($n=1,2,\ldots$). Further technical details of the GW-BSE approach can be found in Ref. 19.

The next step is to consider the derivative couplings τ_{mn}, which occur in Eq. (5). First, we analyze the coupling between the electronic many-body ground state (labeled "0") and an excited state $n \geq 1$. This coupling is given by

$$\tau_{0n} = \langle \Psi_0 | \partial \Psi_n \rangle, \quad (11)$$

where Ψ_0 is the Slater determinant Φ_0^{det} of all the occupied single-particle states. The derivative with respect to nuclear coordinates is abbreviated as ∂. In all further calculations, we take Φ_0^{det} as

$$\Phi_0^{\mathrm{det}}(x_1, \ldots, x_N) = \frac{1}{\sqrt{N!}} \sum_{\mathbb{P} \in S_N} \mathrm{sgn}(\mathbb{P}) \psi_{v_1}(x_{\mathbb{P}(1)}) \ldots \psi_{v_N}(x_{\mathbb{P}(N)}). \quad (12)$$

The sum runs over all elements $\mathbb{P}$ of the permutation group S_N, thus acting as the antisymmetrizator operator of the single-particle states ψ. N is the number of occupied states and x denotes both space and spin. The Ψ_n, on the other hand, have the form of

$$|\Psi_n\rangle = \sum_{vc} A_{vc}^n |\Phi_{vc}^{\mathrm{det}}\rangle. \quad (13)$$

$|\Phi_{vc}^{\mathrm{det}}\rangle$ denotes an independent electron-hole pair state, with the hole (electron) from single-particle level $v(c)$. Since we focus on spin-singlet excited states, $|\Phi_{vc}^{\mathrm{det}}\rangle$ can immediately be expressed as

$$|\Phi_{vc}^{\mathrm{det}}\rangle = \frac{1}{\sqrt{2}}(|\Phi_{v\uparrow c\downarrow}^{\mathrm{det}}\rangle - |\Phi_{v\downarrow c\uparrow}^{\mathrm{det}}\rangle). \quad (14)$$

In here, $|\Phi_{v\uparrow c\downarrow}^{\mathrm{det}}\rangle$ denotes a Slater determinant similar to Eq. (12) but with one occupied state (i.e., $v\uparrow$) replaced by an empty state (i.e., $c\downarrow$), referring to an excitation,

$$\Phi_{v_i\uparrow c_j\downarrow}^{\mathrm{det}}(x_1, \ldots, x_N) = \frac{1}{\sqrt{N!}} \sum_{\mathbb{P} \in S_N} \mathrm{sgn}(\mathbb{P}) \psi_{v_1}(x_{\mathbb{P}(1)}) \ldots \psi_{v_i\uparrow}(x_{\mathbb{P}(i)}) \ldots \psi_{c_j\downarrow}(x_{\mathbb{P}(N)}). \quad (15)$$

Correspondingly, τ_{0n} can be written as

$$\tau_{0n} = \left\langle \Phi_0^{\mathrm{det}} | \partial \sum_{vc} A_{vc}^n \Phi_{vc}^{\mathrm{det}} \right\rangle = \sum_{vc} (\partial A_{vc}^n) \langle \Phi_0^{\mathrm{det}} | \Phi_{vc}^{\mathrm{det}} \rangle + \sum_{vc} A_{vc}^n \langle \Phi_0^{\mathrm{det}} | \partial \Phi_{vc}^{\mathrm{det}} \rangle. \quad (16)$$

Here we assume explicitly that both the coefficients A and the determinants Φ depend on the reaction coordinate, upon which we differentiate with the operator ∂. Analyzing Eq. (16) further we recognize that in the first sum, $\langle \Phi_0^{\mathrm{det}} | \Phi_{vc}^{\mathrm{det}} \rangle = 0$ for all vc simply from orthogonality of the single-particle states from which the Slater determinants are constructed. In the second sum, $\langle \Phi_0^{\mathrm{det}} | \partial \Phi_{vc}^{\mathrm{det}} \rangle$ contains the derivative of two electron-hole-pair Slater determinants [see Eq. (14)] with respect to the reaction coordinate. After some algebra, which fully retains the spin, Eq. (16) finally simplifies to

$$\tau_{0n} = \sqrt{2} \sum_{vc} A_{vc}^n \langle \psi_v | \partial \psi_c \rangle \quad (17)$$

since the scalar product between one Slater determinant and (the derivative of) another results from the scalar products of the contributing single-particle states (or their derivatives). To be more precise, the ψ_v and the ψ_c wave functions appearing here are the single-particle states in which at fixed v and c both determinantal structures differ, and the factor $\sqrt{2}$ is due to spin [cf. Eq. (14)].

Finally, we consider the derivative coupling τ_{mn} between two excited singlet states m and n,

$$\tau_{mn} = \langle \Psi_m | \partial \Psi_n \rangle. \quad (18)$$

Similar to τ_{0n}, the τ_{mn} (with $m \geq 1$) can be written as

$$\tau_{mn} = \left\langle \Psi_m | \partial \sum_{vc} A_{vc}^n \Phi_{vc}^{\mathrm{det}} \right\rangle = \sum_{v'c'} \sum_{vc} A_{v'c'}^{*m} (\partial A_{vc}^n) \langle \Phi_{v'c'}^{\mathrm{det}} | \Phi_{vc}^{\mathrm{det}} \rangle + \sum_{v'c'} \sum_{vc} A_{v'c'}^{*m} A_{vc}^n \langle \Phi_{v'c'}^{\mathrm{det}} | \partial \Phi_{vc}^{\mathrm{det}} \rangle \quad (19)$$

and can be immediately simplified to the following many-particle form:

$$\tau_{mn} = \sum_{vc} A_{vc}^{*m} \partial A_{vc}^n + \sum_{v'c'} \sum_{vc} A_{v'c'}^{*m} A_{vc}^n \langle \Phi_{v'c'}^{\mathrm{det}} | \partial \Phi_{vc}^{\mathrm{det}} \rangle. \quad (20)$$

The evaluation of Eq. (20) in terms of single-particle quantities is a little bit more complicated than Eq. (17), mostly because of the second term which contains nontrivial quadruple sum of integrals $\langle \Phi_{v'c'}^{\mathrm{det}} | \partial \Phi_{vc}^{\mathrm{det}} \rangle$. nonetheless, after some straightforward algebra we find that the nonvanishing components can be symmetrically summed up, resulting in the following final expression for τ_{mn}:

$$\tau_{mn} = \sum_{vc} A^{*m}_{vc}\, \partial A^{n}_{vc} + \sum_{v_i} \sum_{c_j} \sum_{c_l} A^{*m}_{v_i c_j} A^{n}_{v_i c_l} \langle \psi_{c_j} | \partial \psi_{c_l} \rangle - \sum_{v_i} \sum_{c_j} \sum_{v_k} A^{*m}_{v_i c_j} A^{n}_{v_k c_j} \langle \psi_{v_i} | \partial \psi_{v_k} \rangle. \quad (21)$$

Similar to Eq. (17), this final expression for the derivative coupling is completely given by integrals of the contributing single-particle wave functions and their derivatives with respect to the nuclear coordinates. It should be noted that for many systems (including the one studied in this work), the wave functions ψ_j of the quasiparticle states are nearly identical to the Kohn-Sham orbitals resulting from the underlying DFT calculation, which we employ for the calculation of τ_{mn} throughout this paper.

III. NUMERICAL RESULTS

Here we present our numerical results on adiabatic and diabatic lowest singlet excited states of the retinal chromophore PSBR. In detail we analyze their behavior as a function of the twist angle of the photoisomerization process from all-*trans* to 13-*cis*. First, we perform a standard DFT calculation of the all-*trans* isomer of PSBR within the local-density approximation. After geometry relaxation, the Kohn-Sham eigenstates enter the GW-BSE calculation. All single-particle eigenstates, including the Kohn-Sham and quasiparticle wave functions, are expanded in atom-centered Gaussian-orbital basis functions.[20] The elements of the Gaussian basis have the following Cartesian form:

$$\phi_{ijk}(\mathbf{r}) = N_{ijk} x^i y^j z^k e^{-\alpha \mathbf{r}^2}, \quad (22)$$

of which the orbitals of s, p, d, and s^* symmetry type for each individual atom are taken into account. We take four decay constants α for the carbon and nitrogen atoms, with the values 0.2, 0.5, 1.25, and 3.2. For hydrogen, we take three decay constants with the values 0.1, 0.4, and 1.5. This yields a basis size of 1840 for the whole molecule. The basis set contains both localized and more extended orbitals, thus describing both the wave-function behavior near the nuclei and their decay into vacuum equally well. We have checked that below the vacuum level, the single-particle Kohn-Sham eigenvalues resulting from this basis agree with those of a converged plane-wave basis to within 0.1 eV. Above the vacuum level, this comparison becomes difficult to quantify since the plane-wave expansion would simply reflect the periodicity of the supercell. Nonetheless, the Gaussians yield the local density of states above the vacuum level with high accuracy, as well, and the convergence behavior of the electron-hole excited states with respect to the Gaussians proves that all relevant physics above the vacuum level is well represented by our basis.

In order to guarantee convergence of the dielectric function and the self-energy of the subsequent GW calculation, this calculation has been performed with all 1840 states, meaning that the number of empty states included is 30 times larger than the number of occupied states (retinal has 60 occupied levels). In the BSE calculation, we incorporate the upper 50 of the 60 occupied (hole) states, as well as the lowest 190 of the unoccupied (electron) states. This means that 9690 free particle-hole transitions $|vc\rangle$, between all single-particle states from $E_{\mathrm{HOMO}}-12$ eV to $E_{\mathrm{LUMO}}+15$ eV, for all values of the twist angle of the photoisomerisation reaction, are included in the BSE-TDA Hamiltonian, leading to a convergence of Ω_n of better than 0.1 eV for $n=1$ and 2. Further technical details of the GW-BSE-TDA can be found in Ref. 21.

TABLE I. Excitation energies of the all-*trans* isomer of PSBR. All values are in electron volt.

Method	S_0-S_1	S_0-S_2	Ref.
Expt.	2.00	3.22	22
CASPT2	2.07	2.85	23
TDDFT	2.39	3.24	24
TDDFT-TDA	2.63	3.40	25
GW-BSE-RPA[a]	2.07	3.08	This work
GW-BSE-TDA[b]	2.66	3.28	This work

[a]Using GW-BSE at the RPA level.
[b]Using GW-BSE at the TDA level, i.e., forward time propagation only.

Our BSE-TDA results for the all-*trans* isomer of the PSBR molecule yield excitation energies of 2.66 and 3.28 eV for the S_1 and S_2 singlet excited states. In addition to BSE-TDA, we also carry out a BSE-RPA calculation, i.e., including resonant-antiresonant coupling (see the discussion in Sec. II B), with dynamical screening of the electron-hole interaction kernel K and the same particle-hole basis elements $|vc\rangle$ (for details see Ref. 19). The BSE-RPA excitation energies are correspondingly 2.07 and 3.08 eV with a very good agreement (to within ~0.1 eV) with experiment.[22] In Table I, we compile our results and available data from the literature. These data can by further supplemented by a very detailed study of several retinal structures as presented by Lee and co-workers.[26] Our BSE-TDA excitation energy of S_2 agrees very well with a very recent photoabsorption experiments of Nielsen *et al.*[22] The BSE-TDA excitation energy of the S_1 state appears to be overestimated by about 0.6 eV, which we attribute to the use of the Tamm-Dancoff approximation. In Ref. 27, some of us have reported relatively big values for the matrix elements of the particle-hole interaction kernel K within full RPA treatment, where one allows for unlimited number of particle-hole pairs propagating in both time directions. One can also associate this disagreement between TDA and RPA to the fact that TDA is the limiting case of RPA for the case when the particle-hole interaction K is small compared to the poles of the one-particle propagators G_1. Apparently, in the case of the S_1 excitation of PSBR this condition might not be fulfilled due to the specific chemical nature of the large photoactive orbitals from which S_1 is formed. A time-dependent density-functional theory (TDDFT) calculation by Tachikawa *et al.*[24] (also performed beyond the TDA) shows a slightly worse agreement with experiment than GW-BSE-RPA. Interestingly, the Tamm-Dancoff approximation to the TDDFT (Ref. 28) (TDDFT-TDA) shows effects very similar to our BSE-TDA data.

Starting from the all-*trans* isomer geometry, we calculate

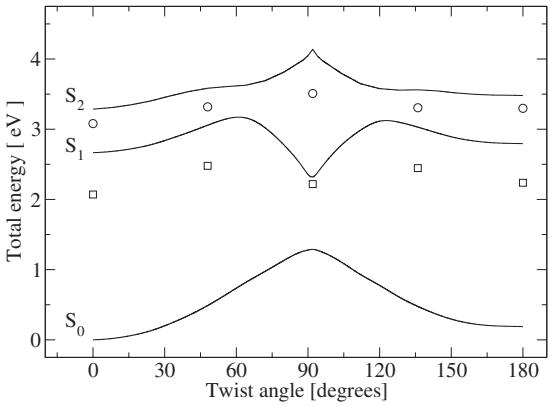

FIG. 3. Adiabatic potential-energy surfaces of the retinal chromophore, calculated along the twist angle from Fig. 1. S_0 denotes the electronic ground state. All energies are with respect to the ground-state energy at 0°. The solid lines for S_1 and S_2 represent BSE-TDA results while the empty squares and empty circles denote BSE-RPA results, i.e., including resonant-antiresonant coupling (see text and Table I).

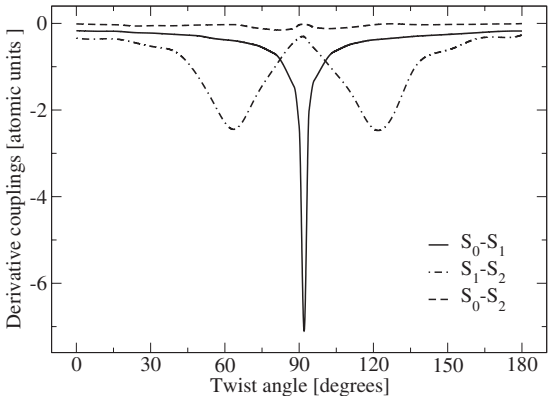

FIG. 4. Derivative couplings between the three states S_0, S_1, and S_2 shown in Fig. 3.

the BSE-TDA PESs for the ground state S_0 and the S_1 and S_2 states along the twist angle of the photoisomerization reaction (see Fig. 3). The ground-state PES increases gradually up to the active region of the photoisomerization reaction at around 92° and then decreases up to 180° (which corresponds to the 13-*cis* isomer). The configuration at 0° is also more stable (by 0.2 eV) than the one at 180°. The S_1 PES, on the other hand, is not really repulsive near the 0° geometry but rather relatively flat. With increasing angle it overpasses a maximum at around 60°, thus forming a potential well of about 0.3 eV depth. These results do support the three-state model of the photoisomerization reaction, as visible in Fig. 3, the torsional movement passes through the avoided-crossing point between the PESs of S_1 and S_2 at about 60° before the twisted conformation at the second avoided crossing (this time between S_1 and S_0) is reached at about 92°. While our calculation of the position of the highest-energy barrier point at 60° agrees with the results by Tachikawa *et al.*,[24] who report it to be 58°, we are not aware of an experimentally derived position of this point. It should be noted, however, that our calculations of PSBR in the gas phase with the saturation by a methyl group cannot be strictly compared to experiments in which the PSBR is connected through the amino group to the protein. Our calculated depth of about 0.3 eV can be also compared with the TDDFT results of Tachikawa *et al.* who find it to be about 0.53 eV. The experimental value for the depth of this well (for PSBR bound to the protein) is found to be about 0.043 eV.[29]

We also checked that along the twist angle, the S_1 excited state is composed mainly (i.e., to about 90–95 %) of the HOMO→LUMO transition (T1), accompanied by some contribution (of about 5%) of HOMO−1→LUMO+1 (T2) The S_2 state, on the other hand, is composed of the HOMO−1→LUMO transtition (T3) (to about 70–90 %) and of the HOMO→LUMO+1 transition (T4) (to about 5–20 %). However, a closer analysis of the states (and, in particular, of their A_{vc} coefficients) reveals an interesting feature. While the T1 and T3 transitions rather maintain their dominant character in both excited states S_1 and S_2 as the twist angle is changed, the coefficients of the T2 and T4 transition tend to undergo an exchange between states S_1 and S_2 in the vicinity of the expected avoided-crossing points at about 60° and 120°. This provides a first understanding of the expected nonadiabatic effects between the many-body electronic states in the retinal molecule. It seems that the adiabatic wave functions of S_1 and S_2 do not interchange fully their character at the avoided-crossing points, which is in distinction to the chemical reactions involving the bond fission processes.[30] Instead, the two states rather become an admixture of each other as the twist angle passes through 60° (and again near 120°). The fact that both states become an admixture of each other or interchange their character completely simply means that they are coupled to each other. If one calculates the matrix elements of the nuclear kinetic-energy operator in the adiabatic representation (or, equivalently, the derivative couplings τ in the diabatic representation, as showed in Fig. 4), one will see that they are nonzero in the vicinity of the avoided-crossing points. Similar effects are to be expected for the avoided crossing between S_0 and S_1 near 90°. This, however, requires a different analysis since in our method the ground state S_0 (i.e., one Slater determinant, resulting from DFT data) and the excited states (i.e., linear combinations of two determinants, resulting from GW-BSE data; see above) are conceptually different.

Before analyzing the nonadiabatic effects in more detail, we briefly investigate the effects of the Tamm-Dancoff approximation at various twist angles. Taking into account the disagreement between BSE-TDA results and experiment, and the much better quality of the BSE-RPA for the all-*trans* isomer at 0°, we have also carried out BSE-RPA calculations at selected configurations of 48°, 92°, 136°, and 180°. These results are included in Fig. 3 as empty symbols. The difference between RPA and TDA results for the S_1 state is larger at 0° than in the most active area of the reaction coordinate (near 90°). This corresponds to our observation that the two excited states (as well as the S_0 state) change their character due to nonadiabatic effects as the twist angle increases. These findings nonwithstanding, our calculations indicate that the allover behavior of the BSE-TDA data as a function of twist angle is very similar to the BSE-RPA results. There-

fore, the following discussion of nonadiabatic effects is carried out for the BSE-TDA data, only. The analysis of diabatic coupling among the BSE-RPA states would be significantly more difficult than the formalism outlined in Sec. II B. We believe that our findings also reflect nonadiabatic behavior of retinal to be expected from the BSE-RPA framework.

Based on the BSE-TDA results, we perform a diabatic transformation of the states S_0, S_1, and S_2 as described in Sec. II A. First, we calculate the derivative couplings τ, as given by Eqs. (17) and (21). This requires to evaluate the derivatives of the Kohn-Sham eigenstates with respect to the twist angle φ, which we realize by finite differences. Since the Kohn-Sham states ψ are represented by Gaussians, i.e., $\psi_\alpha = \Sigma_m C_{m,\alpha}|m\rangle$, the integrals of the form $\langle\psi_\alpha|\partial\psi_\beta\rangle$ can be written at the lowest-order approximation as

$$\langle\psi_\alpha|\partial\psi_\beta\rangle = (1-\delta_{\alpha\beta})(\delta\varphi)^{-1}\sum_{mn} C^*_{m,\alpha}(\varphi)C_{n,\beta}(\varphi+\delta\varphi) \times\langle m(\varphi)|n(\varphi+\delta\varphi)\rangle, \quad (23)$$

i.e., by an unsymmetrical two-point formula for numerical derivatives. Particular care is required when evaluating the integrals $\langle m(\varphi)|n(\varphi+\delta\varphi)\rangle$ between Gaussian basis functions since this overlap is taken between functions at the reference and the shifted geometry. In our calculations, we use a spatial shift of $\delta\varphi=0.1°$, and we sample the whole range of twist angle from 0° to 180° in steps of 6°. All three derivative couplings are plotted in Fig. 4. The solid line is the S_0-S_1 coupling, the dashed line stands for the S_0-S_2 coupling, and dashed-dotted line for S_1-S_2. The nonadiabatic derivative couplings indicate several issues. The coupling between S_0 and S_1 is the most prominent one, with a sharp peak centered around 92°. The coupling between S_1 and S_2 is significantly smaller, being almost symmetrical with respect to $\varphi=92°$, and exhibits maximum values at about 60°–65° and 120°–125°. This could already be expected from the location of the avoided crossings between S_1 and S_2 in the adiabatic picture, as shown in Fig. 3. The S_0-S_2 coupling is close to zero, meaning that these states are only very weakly coupled.

Once all the derivative couplings between states of interest are obtained, one can perform the diabatization transformation by first solving the differential equation, Eq. (5) and then applying Eq. (7). Within the three-state model of photoisomerization one has to perform the diabatization in the space of all three states. In this case, Baer's formula Eq. (5) is a set of three coupled first-order differential equations which can be solved numerically to give all the mixing angles θ at all considered geometries. The final results are shown in Fig. 5. The original adiabatic states are included as dotted lines, and the newly derived states in the diabatic representation are given by the dashed lines.

As expected, the diabatic states clearly exhibit a very smooth behavior with varying twist angle. They also show a very important feature: instead of avoided crossings one gets energies that cross each other at the former avoided-crossing positions. In the case of the three-state diabatization, our diabatic energies do not exactly coincide with their adiabatic analogs after the twist angle has passed the avoided-crossing region.[31,32] This is an effect of being the solution of coupled differential equations with different couplings between each pair. Nonetheless, they are located reasonably with respect to the adiabatic ones. Strict coincidence of the diabatic and adiabatic energies for twist angles of 0° and of 180° can be realized in the case of the two-state diabatization, by putting appropriate boundary conditions on τ. These additional results are showed in Fig. 6.

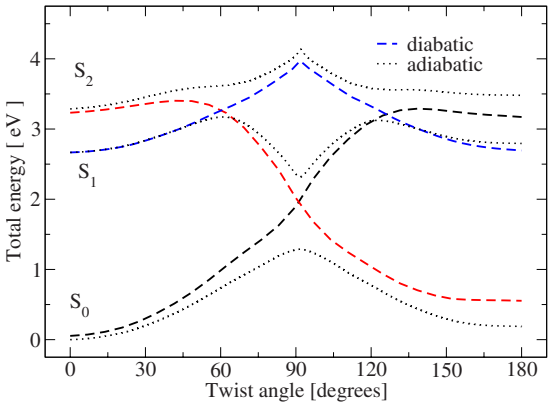

FIG. 5. (Color online) Adiabatic and diabatic BSE-TDA derived electronic states resulting from the derivative couplings of Fig. 4 between S_0, S_1, and S_2. The dotted lines represent the adiabatic states (same as in Fig. 3) and the dashed lines are the diabatic states. All energies are with respect to the ground-state energy at 0°.

Discussing the general properties of the diabatic states, one immediately notices that they fully confirm the expected character of the photoisomerisation reaction in the retinal chromophore. In particular, Fig. 5 exhibits one diabatic surface (I) which connects the all-*trans* ground state S_0 to the 13-*cis* S_2 excited state, and a second diabatic surface (II) connecting the all-*trans* S_2 excited state to the ground state in 13-*cis* configuration. A third surface connects the S_1 all-*trans* to the S_1 13-*cis* state. The existence of the I and II surfaces can be understood within the chemical picture, in which two π-type electrons are lifted from the bonding to antibonding orbital as a result of the molecular torsion by 180°. The diabatic states, as they result here, do not provide a rigorous quantitative description of the photoisomerisation reaction. Nonetheless, the analysis of their behavior can confirm or

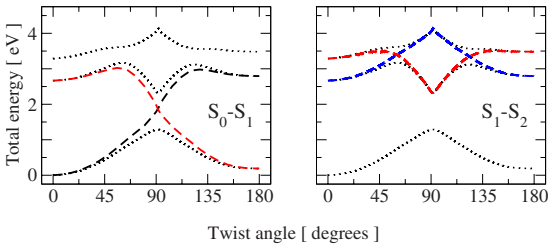

FIG. 6. (Color online) Adiabatic and diabatic BSE-TDA derived electronic states resulting from coupling between only *two* of the three states S_0, S_1, and S_2 (two-state block diabatization). The dotted lines represent the adiabatic states (same as in Fig. 3) and the dashed lines are the diabatic states. The left (right) panel considers coupling between S_0 and S_1 (S_1 and S_2). All energies are with respect to the ground-state energy at 0°.

disprove the chosen reaction model. In the present case, our findings strongly support the three-state model.

Diabatic states and their energies can be used in subsequent time-dependent quantum-wave-packet dynamics.[33,34] Such calculations can be conveniently performed by solving the time-dependent Schrödinger equation for the molecular wave function of Eq. (1) but now expressed in the diabatic representation. Here one propagates effectively a vector of nuclear wave packets in all three diabatic channels S_0, S_1, and S_2 by means of applying the operator $e^{-i\epsilon H}$ to the wave function, with H containing the nondiagonal matrix $\mathbf{V}$ of the electronic Hamiltonian in the diabatic representation. The propagation itself can be done very efficiently by means of a new state-of-the-art high-order factorization operator method.[35] The key answer from the dynamical simulations is then not only the quantum yield for the photoisomerisation but also the prediction of the time needed to pass the S_1-S_2 and S_0-S_1 crossings, and finally the time-resolved photon absorbance spectra for this reaction. All these results depend heavily on the nonadiabatic coupling between the states, on their overall shape, and the position of the avoided-crossing points.

At this point it is important to stress that the diabatic results displayed in Figs. 4–6, have been performed at the TDA level. This means that all the formulas required to derive the nonadiabatic derivative couplings τ, as was discussed in Sec. II B, have assumed the TDA form of the many-body excited state of Eq. (9). As we already discussed, the BSE-RPA calculations resulted in better agreement with experiment than BSE-TDA. Taking a look at Fig. 3 again, it is evident that within BSE-RPA, one may eventually obtain slightly different diabatic states. Apart from the vertical shift of the excited states as a function of the twist angle, there might also be a displacement of the first S_1-S_2 avoided-crossing point (at around 60°) toward smaller twist angle, as well as a displacement of the second S_1-S_2 avoided crossing toward larger twist angle. There are, however, conceptual differences between diabatization of the BSE-TDA and BSE-RPA derived excited states. In particular, the BSE-RPA derived excited state Ψ_n has the following wave-function form:

$$|\Psi_n\rangle = \sum_{vc} (A^n_{vc} a^\dagger_v b^\dagger_c - B^n_{vc} b_c a_v)|0\rangle. \tag{24}$$

This is the typical RPA representation of the many-body wave function.[36] It includes (in addition to the TDA form) a new term containing the b_c and a_v operators, destroying the particle-hole pair in the ground state. Diabatization of the BSE-RPA states would thus require to rederive the diabatization formulas for this particular form of the wave function, which would go far beyond our present work.

IV. CONCLUSIONS

We presented a scheme of evaluating diabatic electronic states which is applicable to molecules, clusters, and periodic systems and allows to obtain the true physical description of nonadiabatic phenomena where the Born-Oppenheimer approximation fails. The diabatization schemes have been for a very long time conducted in the context of quantum-chemical studies. Our approach is the usage in the context of an electronic-structure method from the physics community, i.e., the DFT-GW-BSE method. We demonstrate the applicability of the approach by discussing nonadiabatic effects in the photoisomerization reaction of the retinal chromophore existing in in bacterium *Halobacterium halobium*.

Other possible applications beyond this study are many other light-driven dissociation processes in condensed matter, on surfaces, etc. We consider the calculation of the derivative couplings in the Baer's method as relatively straightforward from a computational point of view within the GW-BSE scheme, which makes the whole approach a rather universal one. Finally, the diabatic states may be used as the input for direct quantum-dynamical simulations, whenever it is important to retain nonadiabatic effects without artificial electronic movements between the potential-energy surfaces such as, e.g., in the surface hopping method.[37]

*mkaczm@gmail.com

[1] G. Wald, Science **162**, 230 (1968).
[2] E. Racker and W. Stoeckenius, J. Biol. Chem. **249**, 662 (1974).
[3] K. C. Hasson, F. Gai, and P. A. Anfinrud, Proc. Natl. Acad. Sci. U.S.A. **93**, 15124 (1996).
[4] T. Kobayashi, T. Saito, and H. Ohtani, Nature (London) **414**, 531 (2001).
[5] R. Govindjee, S. P. Balashov, and T. G. Ebrey, Biophys. J. **58**, 597 (1990).
[6] C. A. Mead and D. G. Truhlar, J. Chem. Phys. **77**, 6090 (1982).
[7] A. Szabo and N. S. Ostlund, *Modern Quantum Chemistry* (McGraw-Hill, USA, 1989).
[8] B. Heumann and R. Schinke, J. Chem. Phys. **101**, 7488 (1994).
[9] T. Pacher, L. S. Cederbaum, and H. Koppel, Adv. Chem. Phys. **84**, 293 (1993).
[10] M. Baer, Chem. Phys. Lett. **35**, 112 (1975).
[11] M. Baer, Phys. Rep. **358**, 75 (2002).
[12] G. Onida, L. Reining, and A. Rubio, Rev. Mod. Phys. **74**, 601 (2002).
[13] E. E. Salpeter and H. A. Bethe, Phys. Rev. **84**, 1232 (1951).
[14] L. J. Sham and T. M. Rice, Phys. Rev. **144**, 708 (1966).
[15] G. Strinati, Phys. Rev. B **29**, 5718 (1984).
[16] L. Hedin, Phys. Rev. **139**, A796 (1965).
[17] F. Aryasetiawan and O. Gunnarsson, Rep. Prog. Phys. **61**, 237 (1998).
[18] A. Fetter and J. D. Walecka, *Quantum Theory of Many-Particle Systems* (Dover, USA, 2003).
[19] M. Rohlfing and S. G. Louie, Phys. Rev. B **62**, 4927 (2000).
[20] P. R. Briddon and R. Jones, Phys. Status Solidi B **217**, 131 (2000).
[21] M. Rohlfing, Int. J. Quantum Chem. **80**, 807 (2000).
[22] I. B. Nielsen, L. Lammich, and L. H. Andersen, Phys. Rev. Lett. **96**, 018304 (2006).
[23] S. Sekharan, O. Weingart, and V. Buss, Biophys. J. **91**, L07

(2006).
[24] H. Tachikawa and T. Iyama, J. Photochem. Photobiol., B **76**, 55 (2004).
[25] M. Sun, Y. Ding, G. Cui, and Y. Liu, J. Phys. Chem. A **111**, 2946 (2007).
[26] H. M. Lee, J. Kim, C.-J. Kim, and K. S. Kim, J. Chem. Phys. **116**, 6549 (2002).
[27] Y. Ma, M. Rohlfing, C. Molteni, and E. M. Gonzalez, J. Chem. Theory Comput. **6**, 257 (2010).
[28] S. Hirata and M. Head-Gordon, Chem. Phys. Lett. **314**, 291 (1999).
[29] R. Gonzalez-Luque, M. Garavelli, F. Bernardi, M. Merchan, M. A. Robb, and M. Olivucci, Proc. Natl. Acad. Sci. U.S.A. **97**, 9379 (2000).
[30] P. W. Kash, G. C. G. Waschewsky, R. E. Moss, L. J. Butler, and M. M. Francl, J. Chem. Phys. **100**, 3463 (1994).
[31] T. Klüner, S. Thiel, and V. Staemmler, J. Phys. B **32**, 4931 (1999).
[32] M. S. Kaczmarski and M. Rohlfing, J. Phys. B **43**, 051001 (2010).
[33] M.-Y. Zhao, Q.-T. Meng, T.-X. Xie, K.-L. Han, and G.-Z. He, Int. J. Quantum Chem. **101**, 153 (2005).
[34] B. Heumann, K. Weide, R. Düren, and R. Schinke, J. Chem. Phys. **98**, 5508 (1993).
[35] S. A. Chin, S. Janecek, and E. Krotscheck, Chem. Phys. Lett. **470**, 342 (2009).
[36] P. G. Reinhard and Y. K. Gambhir, Ann. Phys. **504**, 598 (1992).
[37] N. L. Doltsinis and D. Marx, Phys. Rev. Lett. **88**, 166402 (2002).